Applications of Rare Earth Metal Ion-Embedded Nano Ferrites in Dye Removal from Water

Ashvini V Meshram[1,a], Indrani B Das Sarma[2,b] and Kishor M Hatzade[3,c]

[1] *Department of Chemistry, M. B. Patel College, Deori, Maharashtra, India.*
[2] *Department of applied science and humanities, Jhulelal Institute of Technology, Nagpur, Maharashtra, India.*
[3] *Department of Chemistry, Dhote Bnadhu Science College, Gondia, Maharshtra, India*

[a] ashvinim20@gmail.com
[b] dassarmaindrani@gmail.com
[c] kishorhatzade@gmail.com

Abstract

Nano-ferrites are proved to be a powerful and commendable material nowadays for removal of hazardous pollutants from waste water. Incorporation of rare earth metal ions into these metal ferrites alters the characters of specific metal nano-ferrites. In this study, Lanthanum doped (x=0,0.1,0.3,0.5) cobalt ferrites ($CoLa_xFe_{2-x}O4$) were prepared via sol-gel synthesis. Synthesized doped nano-ferrites were characterized through FTIR, XRD (26.74 nm, 7.66 nm, 39.57 nm and 2.12 nm), SEM-EDX and SEM techniques. The impact of incorporation of lanthanum ions on adsorption efficiency of different nano-ferrites material was checked to the adsorption of methylene blue dye and Rhodamine B dye and the results were compared.

Keywords: Lanthanum Doped Nano-Ferrites; Characterization; Adsorption; Dye Removal Efficiency; Methylene Blue.
Received 31 January 2025; First Review 10 March 2025; Accepted 19 March 2025.

*** Address of correspondence**
Ashvini V Meshram
Department of Chemistry, M. B. Patel College, Deori, Maharashtra, India.

Email: ashvinim20@gmail.com

How to cite this article
Ashvini V Meshram, Indrani B Das Sarma and Kishor M Hatzade, Applications of Rare Earth Metal Ion-Embedded Nano Ferrites in Dye Removal from Water, J. Cond. Matt. 2025; 03 (01): 129-132.

Available from:
https://doi.org/10.61343/jcm.v3i01.133

Introduction

Water body contamination is one of the main issues with environmental degradation that exists today. Because of the presence of multiple contaminations less than 1% of the total water is fit for human consumption [1]. Unusual industrial and population growth led to environmental problems, which prompted scientists to look for cutting-edge materials to adapt to the new environment [2]. Adsorptive removal involves physically removing of pollutant molecules by filtering them after they have been adsorbed on the particle surface. Pollutants that are exposed to light causing electron-hole generation on the particle surface, which initiates electron transfer processes that lead to chemical deterioration through photocatalytic degradation [3].

The most frequent waste that the textile and printing industries discharge into water bodies is dyes. Due to their complicated aromatic structure and resistance to heat, light, and chemicals, these colours biodegrade extremely slowly [4]. These dyes can penetrate the food chain and cause a variety of deadly diseases in humans by way of other living species. They can also produce a large number of secondary products through a sequence of photochemical and physiochemical reactions. Therefore, it is crucial to remove these dangerous pigments from water [5].

Adsorbent materials such as clay, zeolite, metal oxides, activated carbon, and carbon allotropes are frequently utilised in the removal of dyes. Although clay, activated carbon, and metal oxide-based adsorbents have strong adsorption efficiency, their usage is limited by a number of drawbacks, such as the production of sludge, high regeneration costs, the high cost of activated carbon, and the leaching effect's ability to remove metal oxides [6]. Methylene blue (MB) is a substance with a wide range of uses. It is used in the photo-reducible dyes used in galvanic cells in industry, as oxygen detectors in vacuum-packed food items, as an electrochromic material in windows, sun roofs, and rear-view mirrors, as well as staining, bacteriology, and microscopy in medicine. However, when consumed by people, it results in a number of health issues. Because of this, dyes shouldn't be released into natural sources or effluents unless they have first undergone partial or complete elimination procedures [7].

Method

The reagents used in 1:2 ratios to produce the cobalt ferrite through sol-gel synthesis. $Fe(NO_3)_3.9H_2O$, $Co(NO_3)_2.6H_2O$ and Urea were dissolved in 30 mL of deionized water. Three other compositions also were prepared using $La(NO_3)_3.6H_2O$ to produce samples with the formula $CoLa_xFe_{2-x}O_4$, with x values of 0.1, 0.3 and 0.5. In order to obtain the products, the precursors in solution were heated to 85 °C for 3 h under magnetic stirring until a gel was achieved. Subsequently, the gel was dried at microwave oven on 900 volt for 6 minutes, then it was crushed in Morton-piston for 12 hours then it was transferred to an alumina crucible and treated in a muffle furnace at 300 °C for 20 h to ensure the complete decomposition of organics. Finally, the characterization of the black powder was carried out. Crystalline structures of the samples were characterized in an X-ray diffractometer (XRD, Philips, X'pert MPD) equipped with a CuKα source with step size 0.02° and a 2θ range of 10-90 degree. ICSD data banks were used for the identification of the resulting crystalline phases. The shape and morphology of the particles were analysed using scanning electron microscopy (SEM). Fourier transform infrared (FT-IR) spectrum is recorded on Perkin Elmer 2000 FT-IR spectrometer in KBr pellets. EDX is done to confirm the chemical composition of the ferrites. Adsorption of methylene blue dye and Rhodamin B dye is studied by dissolving 0.01 g of ferrites and stir it for 30 minutes. The stock solution of 1 ppm was prepared and 25 Ml was taken for the adsorption study. The adsorption is taken at two different Ph acidic and basic which is adjusted using (0.1 mol/L) HCL and NaOH. The absorbance was recorded for the interval of the 5 minutes on SHIMADZU UV Spectrophotometer, UV-1800.

Discussion

Characterization: In this study, different techniques (FTIR, XRD, EDX-SEM and SEM) were used to characterised the prepared lanthanum doped cobalt ferrites. The FTIR spectrum of synthesised ferrites within the wavelength range 400 to 4000 cm^{-1} is shown in figure 1. In the spectrum, the absorption peaks at 525 cm^{-1} and 446 could be ascribed to stretching vibration of metal-oxygen bond (Fe-O) at octahedral and tetrahedral sites, respectively. These two peaks suggest the formation of spinel ferrite-type oxide [8]. The absorption peak at 1036 cm^{-1} could be attributed to NO_3-group [9]. But this peak is not observed in case on $CoLa_{0.3}Fe_{1.7}O_4$. This indicates the structural changes at the x=0.3 doped ferrite. The observed peak at 2350 cm^{-1} is assigned to the C-H vibration.

Figure 2 displays the XRD patterns of doped ferrites samples made using the sol-gel method. Indexed as (220), (311), (222), (400), (422), (511), (440), (533) and (622) planes, the well-defined peaks that have been detected correspond to a single phase with cubic spinel. The broadening of the peaks is due to nano size of the crystalline particles. The size is calculated using Debey-Sherrer formula and is found that 26.74 nm, 7.66 nm, 39.57 nm and 2.12 nm for $CoLa_xFe_{2-x}O_4$ from x=0, 0.1, 0.3 and x=0.5 respectively. The extra peaks found at for the x =0.3 dopes ferrites. This also indicates the change in the structure of this doped ferrites.

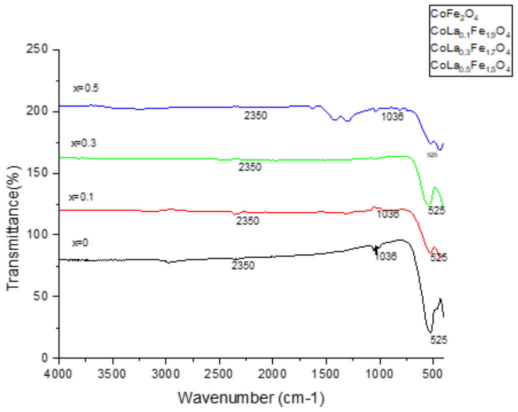

Figure 1: FTIR Spectrum of $CoLa_xFe_{2-x}O_4$ (x=0, 0.1, 0.3, 0.5).

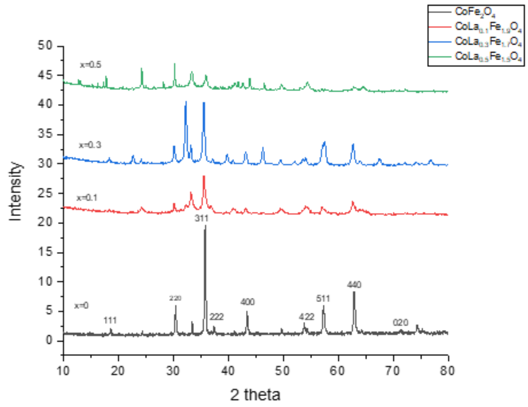

Figure 2: XRD Pattern obtained for $CoLa_xFe_{2-x}O_4$ (x=0.1, 0.3, 0.5).

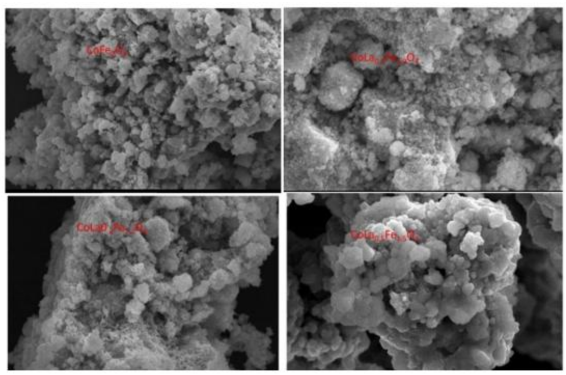

Figure 3: SEM images of $CoLa_xFe_{2-x}O_4$ (x=0, 0.1, 0.3, 0.5).

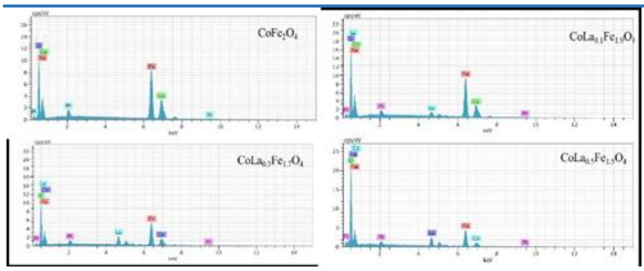

Figure 4: EDX of $CoLa_xFe_{2-x}O_4$ (x=0, 0.1, 0.3, 0.5).

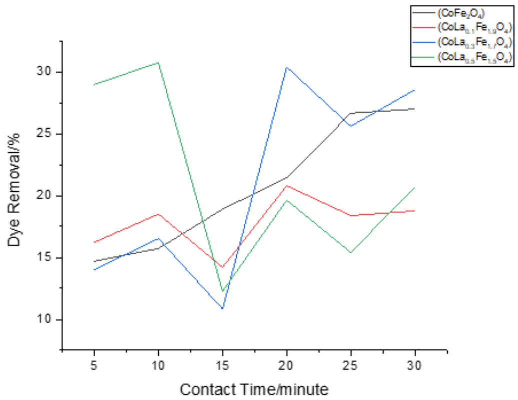

Figure 5: Effect of contact on MB removal percentage (Acidic medium).

Scanning electron microscopy (SEM) wad used to investigate the surface morphology of the synthesised ferrites, as shown in figure 3. As can be seen from the SEM image, the surface of ferrites consists of large grains which are surrounded by small particles. It is observed from the images that for cobalt ferrite x =0.3 doped ferrite the particle is well dispersed but in case of x =0.1 and 0.5 observed the cluster.

The SEM-EDX is shown in the figure 4, this elemental analysis shows the presence of the elements Co, La and Fe. The increased concentration was seen as the increase in height of peaks of Lanthanum from 0.1 to 0.3.

Effect of contact time for MB dye: Figure 5 shows the effect of contact time on the removal percentage of methylene blue. In this experiment, the contact time was changed and the removal percentage increases with time. It is observed that maximum efficiency reached the 30% for $CoLa_{0.3}Fe_{1.7}O_4$. It has been found that with increase in doping percentage of lanthanum contact time of for the adsorption required less in acidic medium. In the basic medium, $CoFe_2O_4$ adsorbed good as compared to the lanthanum doped cobalt ferrites.

Effect of contact time for Rhodamine B dye: Figure 7 shows as the contact time increases the dye removal capacity in acidic medium. The dye removal percentages increase from $CoFe_2O_4$ to $CoLa_xFe_{2-x}O_4$ as the concentration of lanthanum increases. The maximum efficiency is 23.39% for $CoLa_{0.5}Fe_{1.5}O_4$.

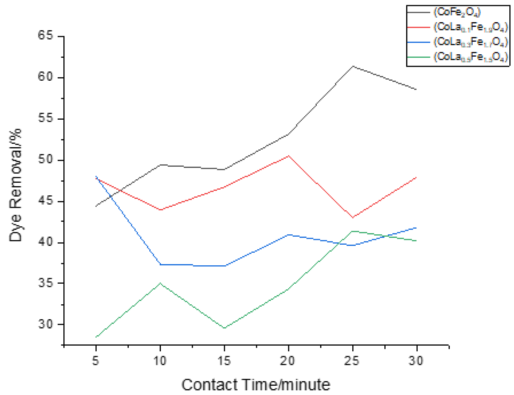

Figure 6: Effect of contact on MB removal percentage (Basic medium).

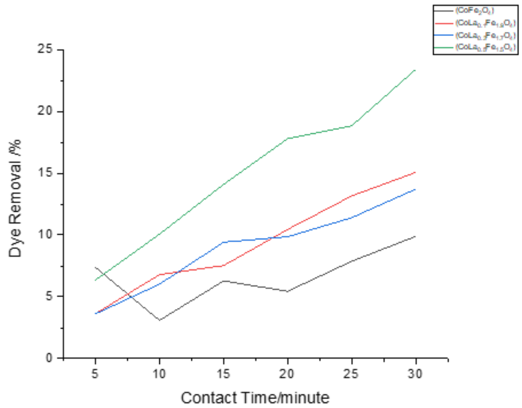

Figure 7: Effect of contact on Rhodamine B removal percentage (Acidic medium).

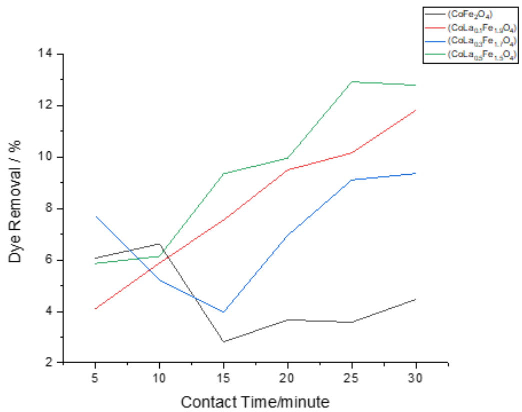

Figure 8: Effect of contact on Rhodamine B removal percentage (Basic medium).

Figure 8 shows the dye removal % in basic medium. It is observed that with increase in contact time % removal increases. Also, with increase in the doping concentration % removal increased.

Conclusion and Future Prospective

In summary, the ferrites $CoLa_xFe_{2-x}O_4$ where x=0, 0.1, 0.3, 0.5 synthesised successfully. Dye removal efficacy increases with increase in contact time and increase with lanthanum doping in case of Rhodamine B dye in acidic and basic medium with maximum efficiency reached to 23.29 %. in case of methylene blue dye with increase in contact time dye removal % increase but the maximum efficiency is found for $CoLa_{0.3}Fe_{1.7}O_4$. This is due to the structural changes found in this ferrite. Comparing the acidic and basic medium dye removal %, in methylene blue dye in acidic medium removal is less as compared to basic one. In case of Rhodamine B dye, in acidic medium the dye removal % is more as compared to the basic medium.

This result can be used to waste water treatment release from industries. The water may be acidic or basic depending upon the which type of industry, so the both acidic and basic medium results are helpful form the purification of water.

References

1. Mariosi, Fabricio Ravanello et al, *"Lanthanum-doped spinel cobalt ferrite ($CoFe_2O_4$) nanoparticles for environmental applications"*, Ceramics International 46.3 (2020): 2772-2779.
2. Keerthana, S. P. et al, *"Synthesis of pure and lanthanum-doped barium ferrite nanoparticles for efficient removal of toxic pollutants"*, Journal of Hazardous Materials 424 (2022): 127604.
3. Singh, Somendra, Yogendra Yadawa, and Amit Ranjan, *"Enhanced adsorption of methylene blue by mixed-phase bismuth ferrite prepared by non-aqueous sol-gel route"*, Journal of Environmental Chemical Engineering 11.1 (2023): 109229.
4. Chahar, Deepika et al, *"Visible light induced photocatalytic degradation of methylene blue dye by using Mg doped Co-Zn nanoferrites"*, Materials Research Bulletin 162 (2023): 112205.
5. Haider, Sajjad et al, *"Visible light active Cu-doped iron oxide for photocatalytic treatment of methylene blue"*, Ceramics International 48.6 (2022): 7605-7612.
6. Abbasi, Muhammad Ali et al, *"Congo red removal by lanthanum-doped bismuth ferrite nanostructures"*, Journal of Physics and Chemistry of Solids 170 (2022): 110964.
7. Cabrera, A. F. et al, *"Degradation of methylene blue dye under dark and visible light conditions in presence of hybrid composites of nanostructured $MgFe_2O_4$ ferrites and oxygenated organic compounds"*, Journal of Environmental Chemical Engineering 8.5 (2020): 104274.
8. Kumar L., Kumar P., Kar M.J. Alloy. Compounds, 2013, 551:72.
9. Konicki, Wojciech, et al, *"Equilibrium and kinetic studies on acid dye Acid Red 88 adsorption by magnetic $ZnFe_2O_4$ spinel ferrite nanoparticles"*, Journal of colloid and interface science 398 (2013): 152-160.
10. Zhao, Xiruo, et al, *"Synthesis and characterization of gadolinium doped cobalt ferrite nanoparticles with enhanced adsorption capability for Congo Red"*, Chemical Engineering Journal 250 (2014): 164-174.
11. Keerthana, S. P., et al, *"Pure and Ce-doped spinel $CuFe_2O_4$ photocatalysts for efficient rhodamine B degradation"*, Environmental Research 200 (2021): 111528.
12. Juna, Byung-Moon, et al, "Accelerated photocatalytic degradation of rhodamine B over carbonate-rich lanthanum-substituted zinc spinel ferrite assembled reduced graphene oxide by ultraviolet (UV)-activated persulfate",
13. Abdo, M. A., Reem Al-Wafi, and M. S. AlHammad, *"Highly efficient visible light driven photocatalytic activity of rare earth cerium doped zinc-manganese ferrite: Rhodamine B degradation and stability assessment"*, Ceramics International 49.17 (2023): 29245-29258.
14. Samoila, Petrisor, et al, *"Boosting catalytic wet-peroxide-oxidation performances of cobalt ferrite by doping with lanthanides for organic pollutants degradation"*, Journal of Environmental Chemical Engineering 9.1 (2021): 104961.
15. Jamaludin, N., et al, *"Photocatalytic degradation of rhodamine B dye under visible light using cerium-cobalt co-doped bismuth ferrite nanoparticles"*, Journal of Physics: Conference Series. Vol. 2432. No. 1. IOP Publishing, 2023.
16. Pardhi, Khushboo T., et al, *"Ionizing Radiation Induced Structural Modification in Nanoferrites"*, (2024).